JACC: BASIC TO TRANSLATIONAL SCIENCE VOL. ■, NO. ■, 2021
© 2021 PUBLISHED BY ELSEVIER ON BEHALF OF THE AMERICAN COLLEGE OF CARDIOLOGY FOUNDATION. THIS IS AN OPEN ACCESS ARTICLE UNDER THE CC BY-NC-ND LICENSE (http://creativecommons.org/licenses/by-nc-nd/4.0/).

PRECLINICAL RESEARCH

High-Fat Diet Enhances Neutrophil Adhesion in LDLR-Null Mice Via Hypercitrullination of Histone H3

Mizuko Osaka, PhD,[a,b] Michiyo Deushi, MS,[a] Jiro Aoyama, MD,[a,c] Tomoko Funakoshi, PhD,[d,e] Akihito Ishigami, PhD,[d] Masayuki Yoshida, MD[a]

VISUAL ABSTRACT

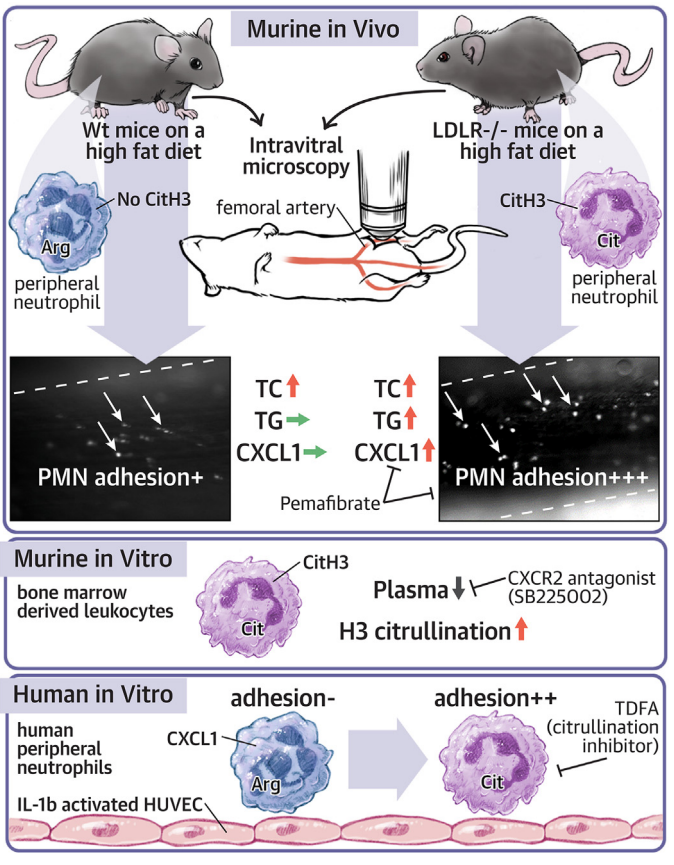

Osaka, M. et al. J Am Coll Cardiol Basic Trans Science. 2021;■(■):■-■.

HIGHLIGHTS

- Neutrophil adhesion to the vascular endothelium in the femoral artery of low-density lipoprotein receptor-null mice fed with HFD was significantly enhanced compared with wild-type mice fed with HFD or low-density lipoprotein receptor-null mice fed with NC.
- HFD induced citrullinated histone H3 of neutrophils in LDL receptor-null mice through the up-regulation of CXCL1 in blood.
- Hypercitrullination of histone H3 in neutrophils by CXCL1 enhanced neutrophil adhesion in vitro and in vivo.
- Pemafibrate decreased neutrophil adhesion and citrullination of histone H3 through the reduction of CXCL1.

From the [a]Department of Life Science and Bioethics, Graduate School of Medical and Dental Sciences, Tokyo Medical and Dental University, Tokyo, Japan; [b]Department of Nutrition and Metabolism in Cardiovascular Disease, Graduate School of Medical and Dental Sciences, Tokyo Medical and Dental University, Tokyo, Japan; [c]Department of Neurosurgery, Graduate School of Medical and Dental Sciences, Tokyo Medical and Dental University, Tokyo, Japan; [d]Research Team for Functional Biogerontology, Tokyo Metropolitan Institute of Gerontology, Tokyo, Japan; and the [e]Department of Physiology, Juntendo University Graduate School of Medicine, Tokyo, Japan.

ISSN 2452-302X https://doi.org/10.1016/j.jacbts.2021.04.002

ABBREVIATIONS AND ACRONYMS

BM = bone marrow

BW = body weight

DNaseI = deoxyribonuclease I

eGFP = enhanced green fluorescent protein

GM-CSF = granulocyte-macrophage colony-stimulating factor

HFD = high-fat diet

HUVECs = human umbilical vein endothelial cells

IVM = intravital microscopy

LDLR = low-density lipoprotein receptor

LysM = lysosome M

MPO = myeloperoxidase

NC = normal chow

NE = neutrophil elastase

NET = neutrophil extracellular trap

PAD4 = peptidylarginine deiminase 4

PPAR = peroxisome proliferator-activated receptor

TC = total cholesterol

TDFA = *N*-acetyl-L-threonyl-L-α-aspartyl-*N*5-(2-fluoro-1-iminoethyl)-L-ornithinamide trifluoroacetate salt

TG = triglyceride

wt = wild type

SUMMARY

Neutrophil adhesion on the atheroprone femoral artery of high-fat diet–fed low-density lipoprotein receptor–null mice was enhanced more than in wild-type mice. The inhibition of histone H3 citrullination of neutrophils reversed the enhancement of neutrophil adhesion, suggesting that hypercitrullination contributes to enhanced neutrophil adhesion. Furthermore, pemafibrate reduced the citrullination of histone H3 in these mice. Therefore, the hypercitrullination of histone H3 in neutrophils contributes to atherosclerotic vascular inflammation. (J Am Coll Cardiol Basic Trans Science 2021;■:■–■) © 2021 Published by Elsevier on behalf of the American College of Cardiology Foundation. This is an open access article under the CC BY-NC-ND license (http://creativecommons.org/licenses/by-nc-nd/4.0/).

Excess fat intake and subsequent dyslipidemia are risk factors for atherosclerosis (1–4). Several studies have shown that vascular inflammation, the principal mechanism that causes atherosclerosis, is connected to a high-fat diet (HFD) or dyslipidemia (5–7). In a previous study, we reported that HFD induces neutrophil adhesion to the arterial vascular endothelium in wild-type (wt) mice (8). The observed neutrophil adhesion was induced by the increase of complement factor C5a, a key modulator in the complement system. Our result uncovered novel transition machinery that links acute inflammation to chronic inflammation in the context of HFD-induced vascular inflammation and sheds light on neutrophils as dominant players in this process (9–11). However, we have not been able to demonstrate the involvement of neutrophils in vascular inflammation associated with atherosclerotic lesion formation because wt mice are resistant to lesion formation after HFD feeding (12). Moreover, the roles of neutrophils, which are key players in acute inflammation in atherosclerosis, have not been thoroughly investigated. Therefore, this study examined the involvement of neutrophils in vascular inflammation associated with atherosclerosis. Furthermore, we hypothesized that differences in HFD-induced neutrophil activation between wt and atherosclerotic mice may influence atherosclerosis-related vascular inflammation. Therefore, this study sought to investigate the detailed mechanism underlying how neutrophils contribute to HFD-induced vascular inflammation in models of atherosclerosis such as low-density lipoprotein recptor-null (LDLR-/-) mice (13–15).

Recent reports highlight an emerging role of neutrophil extracellular traps (NETs) in various neutrophil activation processes such as protection against infection (16) and adhesion of platelets to induce deep vein thrombosis (17,18). NETs have been shown to be initiated by a disruption of chromatin structure in the nucleus through histone citrullination (19). The citrullination of histone is mediated by peptidylarginine deiminase 4 (PAD4), a member of the PAD family of enzymes (20,21). Activated PAD4 converts arginine residues to the citrulline residues of the histone, which triggers the conformational change of the histone complex. More recent studies have identified the involvement of citrullination in various pathophysiological phenomena, such as gene transcription (22) and cell proliferation (23).

1Citrullination or NETs are induced by oxidative stress, lipopolysaccharides, and *N*-formyl-methionyl-leucyl-phenylalanine (24). However, the involvement of lipid components in the citrullination of histones in neutrophils is not well known. Dyslipidemia, such as hypertriglyceridemia and hypercholesterolemia, causes vascular inflammation and atherosclerosis (25,26). Recently, a novel selective peroxisome proliferator-activated receptor (PPAR) modulator has been shown to have the effect of lowering the triglyceride (TG) level in the blood of humans and rodents through the regulation of fatty acid transport and β-oxidation (27,28). Therefore, we proved the induction of histone citrullination in neutrophils by dyslipidemia using $LDLR^{-/-}$ mice as an animal model.

In this study, we report that HFD-induced vascular inflammation involves the enhancement of citrullination in $LDLR^{-/-}$ mice but not in wt mice. The

The authors attest they are in compliance with human studies committees and animal welfare regulations of the authors' institutions and Food and Drug Administration guidelines, including patient consent where appropriate. For more information, visit the Author Center.

Manuscript received September 29, 2020; revised manuscript received April 6, 2021, accepted April 7, 2021.

underlying mechanism seems to be a CXCL1-CXCR2 signal-mediated neutrophil activation through PAD4-dependent citrullination of histone H3. Our results suggest a novel mechanism that may facilitate the transition from acute to chronic inflammation in atherosclerotic vascular inflammation.

METHODS

ANIMALS. Seven-week-old male wt C57BL/6J (wt) mice were obtained from Charles River Laboratories Japan, Inc. (Yokohama, Japan) Lysozyme M (LysM)-enhanced green fluorescent protein (eGFP) mice were kindly gifted from Dr. Y. Inomata (Kumamoto University) (29). LDLR$^{-/-}$ LysM-eGFP mice were generated from LDLR$^{-/-}$ mice and LysM-eGFP mice. The mice were fed the respective diets and water ad libitum. We decided the inclusion and exclusion criteria before the study, and animals with a significant decrease in body weight or food consumption were excluded from this study. Allocation randomization and experimental blinding were performed in all animal experiments. When we had a post-randomization exclusion, it was reported. We used mixed anesthetic agents, including 0.75 mg/kg body weight (BW) of medetomidine, 4.0 mg/kg BW of midazolam, and 5.0 mg/kg BW of butorphanol by intraperitoneal injection as an anesthetic, and 5 μl of 10% lidocaine hydrochloride was used for analgesia in the injured leg by subcutaneous injection. Cervical dislocation was performed under anesthesia as a sacrifice procedure after experiments. All animal experiments conform to National Institutes of Health guidelines. The experiments adhered to the American Physiological Society (APS) Guiding Principles in the Care and Use of Animals and were approved by the Ethical Committee for Animal Experimentation of Tokyo Medical and Dental University (approval nos. A2019-158C and A2019-223A).

INTRAVITAL MICROSCOPY. The wt, LDLR$^{-/-}$, or LDLR$^{-/-}$ LysM-eGFP mice were started on HFD (1.25% cholesterol and 20% fat) (Sankyo Labo Service Corporation, Inc., Shizuoko, Japan) or normal chow (NC) (CE-2, CLEA Japan, Inc., Tokyo, Japan) at the age of 7 weeks. Intravital microscopy (IVM) was performed on the femoral arteries of wt or LDLR$^{-/-}$ mice fed HFD or NC for 28 days. The observation of leukocyte adhesion in the femoral artery using IVM has been previously described (8,30,31). In brief, mice were anesthetized with pentobarbital or mixed anesthetic agents, including 0.75 mg/kg BW of medetomidine, 4.0 mg/kg BW of midazolam, and 5.0 mg/kg BW of butorphanol by intraperitoneal injection. Then, mice were mechanically ventilated to maintain a normal acid-base balance. Rectal temperature was maintained at 36.0°C to 37.0°C with a heating pad and an infrared heat lamp during the experiment. The left femoral artery at the level of the epigastric branch was visualized with a fluorescent microscope (BX51WI, Olympus, Tokyo, Japan) equipped with a water immersion objective (20×) for 60 seconds. Mice received subcutaneous injection of 10% lidocaine to control pain during observation. All images were recorded using a computer-assisted image analysis program MetaMorph (Molecular Devices, LLC., San Jose, California). The parameters used to characterize the adhesive or rolling interactions of leukocytes have previously been described in detail (8,30,31). Moreover, the duration of adhesion in adhesive or rolling leukocytes (<3.0, 3.0 to 59.9, and ≥60.0 s) was calculated.

MONOCYTE/MACROPHAGE DEPLETION. LDLR$^{-/-}$ LysM-eGFP mice fed HFD for 28 days were administered 12.5 mg/kg BW of clodronate liposomes or control liposome (FormuMax Scientific, Inc., Sunnyvale, California) by intravenous injection to the tail vein, and IVM was performed after 24 h.

IMMUNOHISTOCHEMISTRY FOR CITRULLINATED HISTONE H3 OF CIRCULATING NEUTROPHILS OR BONE MARROW–DERIVED LEUKOCYTES. Circulating neutrophils were isolated from blood harvested by cardiac puncture from mice using anti-Ly-6G MicroBeads (Miltenyi Biotec B.V. & Co. KG, Bergisch Gladbach, Germany) according to the manufacturer's protocol. Bone marrow (BM)-derived leukocytes were harvested from the femurs and tibias of LDLR$^{-/-}$ mice by flushing with 1.5 mmol/L ethylenediaminetetraacetic acid in Hank's Balanced Salt Solution. After centrifugation, 1×10^6 cells were seeded on a poly-L-lysine-coated 22-mm coverslip (32). These cells were incubated in Roswell Park Memorial Institute Media 1640 with 20% each of murine plasma from wt mice fed NC or HFD, LDLR$^{-/-}$ mice fed NC or HFD for 28 days or recombinant mouse CXCL1 (BioLegend, Inc., San Diego, California) for 2 h. Cells were fixed by 4% paraformaldehyde in phosphate-buffered saline (PBS[-]) and stained by anti-citrullinated H3 (Abcam, Cambridge, United Kingdom), PE-antimouse Ly-6G (BioLegend, Inc.) and 4′,6-diamidino-2-phenylindole, followed by observation with a fluorescence microscope. The obtained images were analyzed with Meta Morph. The ratio of citrullinated histone H3-positive, Ly-6G-positive neutrophils in total Ly-6G-positive neutrophils was calculated.

ADMINISTRATION OF CXCL1, CXCR2 ANTAGONIST, TDFA, DNaseI, OR PEMAFIBRATE. A total of 0.3 mg/kg CXCL1 was given to LDLR$^{-/-}$ mice fed NC, and

FIGURE 1 **Neutrophil Adhesion Is Enhanced in LDLR$^{-/-}$ Mice Fed HFD for 28 Days**

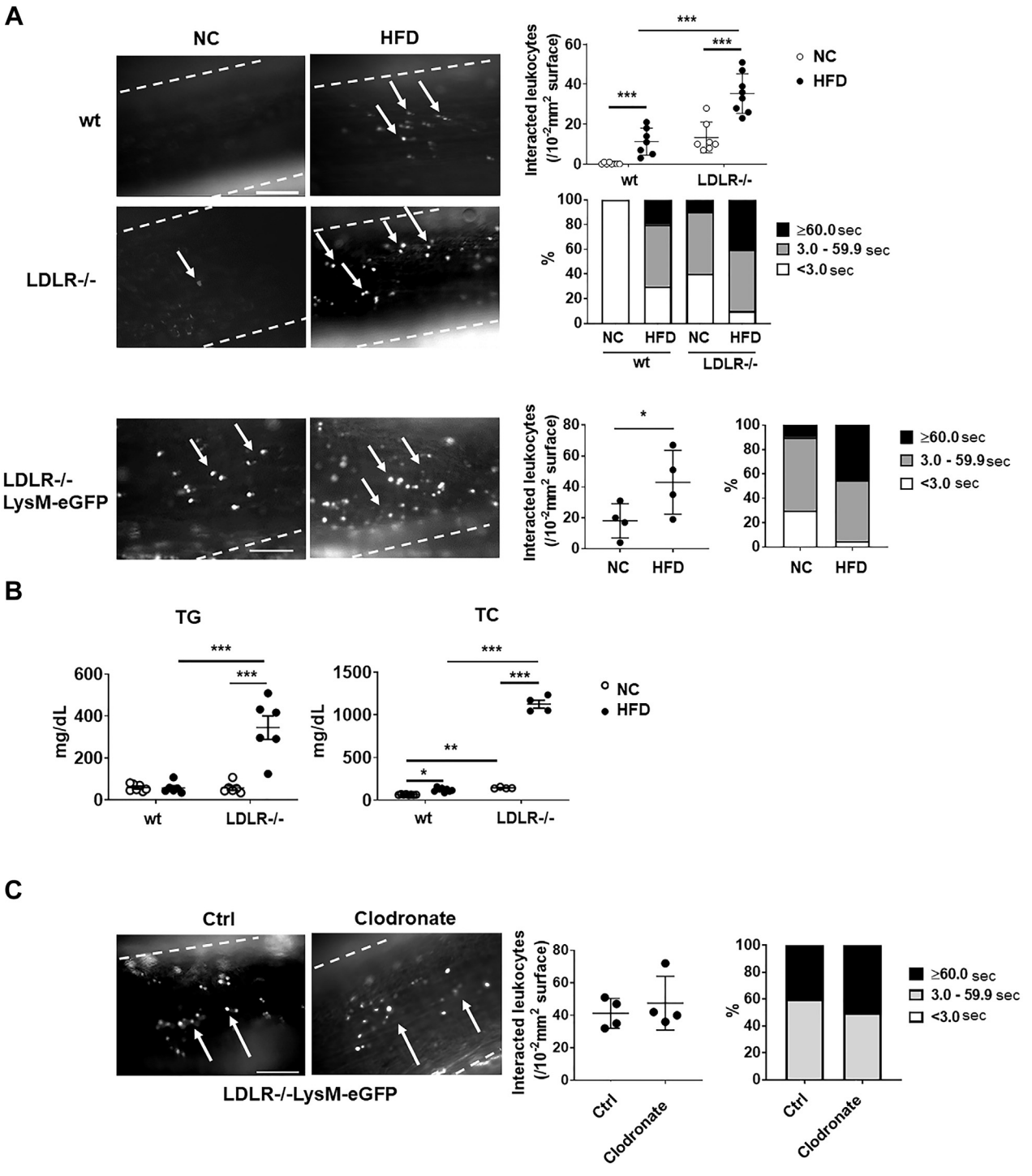

Continued on the next page

circulating leukocytes were isolated after 30 minutes to perform immunohistochemistry for citrullinated histone H3. LDLR$^{-/-}$ mice were fed HFD with or without daily administration of 10 mg/kg BW SB225002 (Cayman Chemical Company, Ann Arbor, Michigan) (33) and 7 mg/kg BW *N*-acetyl-L-threonyl-L-α-aspartyl-*N*5-(2-fluoro-1-iminoethyl)-L-ornithinamide trifluoroacetate salt (TDFA) (Sigma-Aldrich, St. Louis, Missouri) by intraperitoneal injection for 28 days (34). Moreover, 0.2 mg of deoxyribonuclease I (DNaseI, Worthington Biochemical Corporation, Lakewood, New Jersey) was administered to HFD-fed LDLR$^{-/-}$ mice before IVM for 7 days. Furthermore, 0.3 mg/kg BW of pemafibrate (kindly gifted from Kowa Corp. Ltd.) was administered orally for 28 days. Neutrophil adhesion was observed by IVM, and immunohistochemistry for citrullinated histone H3 in BM-neutrophils stimulated by plasma from each mouse was performed.

COMPREHENSIVE CYTOKINE/CHEMOKINE ANALYSIS FOR THE PLASMA OF MICE. Peripheral blood was harvested by cardiac puncture from mice, and plasma was isolated by centrifuge. Comprehensive cytokine/chemokine analysis for the plasma of each mouse was performed using Cytometric Bead Array (BD Biosciences, Franklin Lakes, New Jersey) according to the manufacturer's protocol.

ENZYME-LINKED IMMUNOSORBENT ASSAY. Myeloperoxidase (MPO), neutrophil elastase (NE), and CXCL1 in each mouse plasma were measured by enzyme-linked immunosorbent assay. Blood was obtained by cardiac puncture from wt mice fed NC or HFD for 28 days, and the plasma was isolated. Then, 96-well microplates coated with each captured antibody were blocked by 5% bovine serum albumin in PBS(-) for 1 hour at room temperature, followed by the reaction of samples for 2 h. The microplates were incubated with 100 μl of each antibody for detection for 2 h. After washing, 100 μl of horseradish peroxidase-streptavidin (R&D Systems, Inc., Minneapolis, Minnesota) was added to the microplates and incubated for 30 min, followed by washing. The immunoreaction was developed by adding substrate (Kirkegraad & Perry Laboratoies, Inc., Gaithersburg, Maryland), and 0.3 mol/L H_2SO_4 solution was added to stop the reaction. The absorbance at 450 nm was measured, and the concentration in the samples was calculated using the standard curves. MPO (Hycult Biotech, Uden, the Netherlands), NE (R&D Systems, Inc.), and CXCL1 (R&D Systems, Inc.) were measured according to each manufacturer's protocol.

BLOOD TG AND TOTAL CHOLESTEROL LEVELS. Peripheral blood was harvested by cardiac puncture from mice, and TG and total cholesterol (TC) levels in isolated plasma were measured by cholesterol kit or TG kit (Serotec Co. Ltd., FUJIFILM Wako Pure Chemical Corporation, Osaka, Japan) according to the manufacturer's protocol (Supplemental Table 1).

FLOW CYTOMETRY AND LEUKOCYTE COUNT IN PERIPHERAL BLOOD. Peripheral blood was harvested by cardiac puncture. Rat antimouse CD11b-APC (BioLegend, Inc.), rat antimouse CD45-PerCP (BioLegend, Inc.), and rat antimouse Lymphocyte antigen 6 complex locus G6D (Ly6G)-PE (BioLegend, Inc.) in 1.8 ml of Lysing Buffer (BD Biosciences) were added to 200 μl of blood and incubated for 15 min at room temperature in the dark. After washing, cells were fixed with 1% paraformaldehyde in PBS(-) and analyzed. Flow cytometry analyses were performed for 10,000 cells of single-cell suspension using the BD FACS Caribur, and data were analyzed with FlowJo 7.6 (FlowJo, Ashland, Oregon). Neutrophils were gated at CD45$^+$Ly$^-$6G$^+$CD11b$^+$. The leukocyte count was determined using XT-2000iV (Sysmex, Kobe, Japan).

ISOLATION OF HUMAN CIRCULATING NEUTROPHILS FROM BLOOD. We examined in vitro adhesion assay using human neutrophils to validate neutrophil adhesion. Ethical approval was obtained from ethics committees at Tokyo Medical and Dental University

FIGURE 1 Continued

(A) Leukocyte adhesion on the femoral artery of wt mice, LDLR$^{-/-}$ mice, or LDLR$^{-/-}$ LysM-eGFP mice that specifically express eGFP in neutrophils, fed NC or HFD for 28 days. **Arrowheads** show adhered leukocytes or rolling leukocytes on the vessel wall, and **dashed lines** indicate the vessel wall in the snapshot. Scale bar: 50 μm. **The graph** shows the number of adhered/rolling leukocytes in each mouse **(right)**. **White circles** indicate NC-fed mice, and **black circles** indicate HFD-fed mice. Data are presented as the mean ± SEM. ***$p < 0.001$ and *$p < 0.05$ by 2-way ANOVA with the Bonferroni post hoc test. n = 7 or 8. Videos 1 to 6 show adhered and rolling leukocytes on the femoral artery of each mouse on in vivo imaging. **(B)** TG and total TC levels in the blood of LDLR$^{-/-}$ mice fed HFD for 28 days. TG and TC levels in LDLR$^{-/-}$ mice fed HFD significantly increased compared to wt mice fed HFD or LDLR$^{-/-}$ mice fed NC. **White circles** indicate NC-fed mice, and **black circles** indicate HFD-fed mice. Data are presented as the mean ± SEM. **$p < 0.01$ and *$p < 0.05$ by 2-way ANOVA with the Bonferroni post hoc test. n = 4 or 6. **(C)** Leukocyte adhesion on the femoral artery of LDLR$^{-/-}$ LysM-eGFP mice fed HFD under monocyte/macrophage depletion. Clodronate liposome did not change. **Arrowheads** show adhered/rolling leukocytes or rolling leukocytes on the vessel wall, and dashed lines indicate the vessel wall in a snapshot. Scale bar: 50 μm. **The graph** shows the number of adhered leukocytes in each mouse **(right)**. Data are presented as the mean ± SEM, by unpaired 2-tailed Student's *t*-test (n = 4 in each group). Videos 5 **and** 6 show adhered and rolling leukocytes on the femoral artery of HFD-fed LDLR$^{-/-}$ LysM-eGFP mice with control liposome or clodronate liposome on in vivo imaging.
ANOVA = analysis of variance; Ctrl = control liposome; eGFP = enhanced green fluorescent protein; HFD = high-fat diet; LDLR = low-density lipoprotein receptor; LysM = lysosome M; NC = normal chow; sec = seconds; SEM = standard error of the mean; TC = total cholesterol; TG = triglyceride; wt = wild-type.

FIGURE 2 Citrullination of Histone H3 Is Enhanced in LDLR$^{-/-}$ Mice Fed HFD

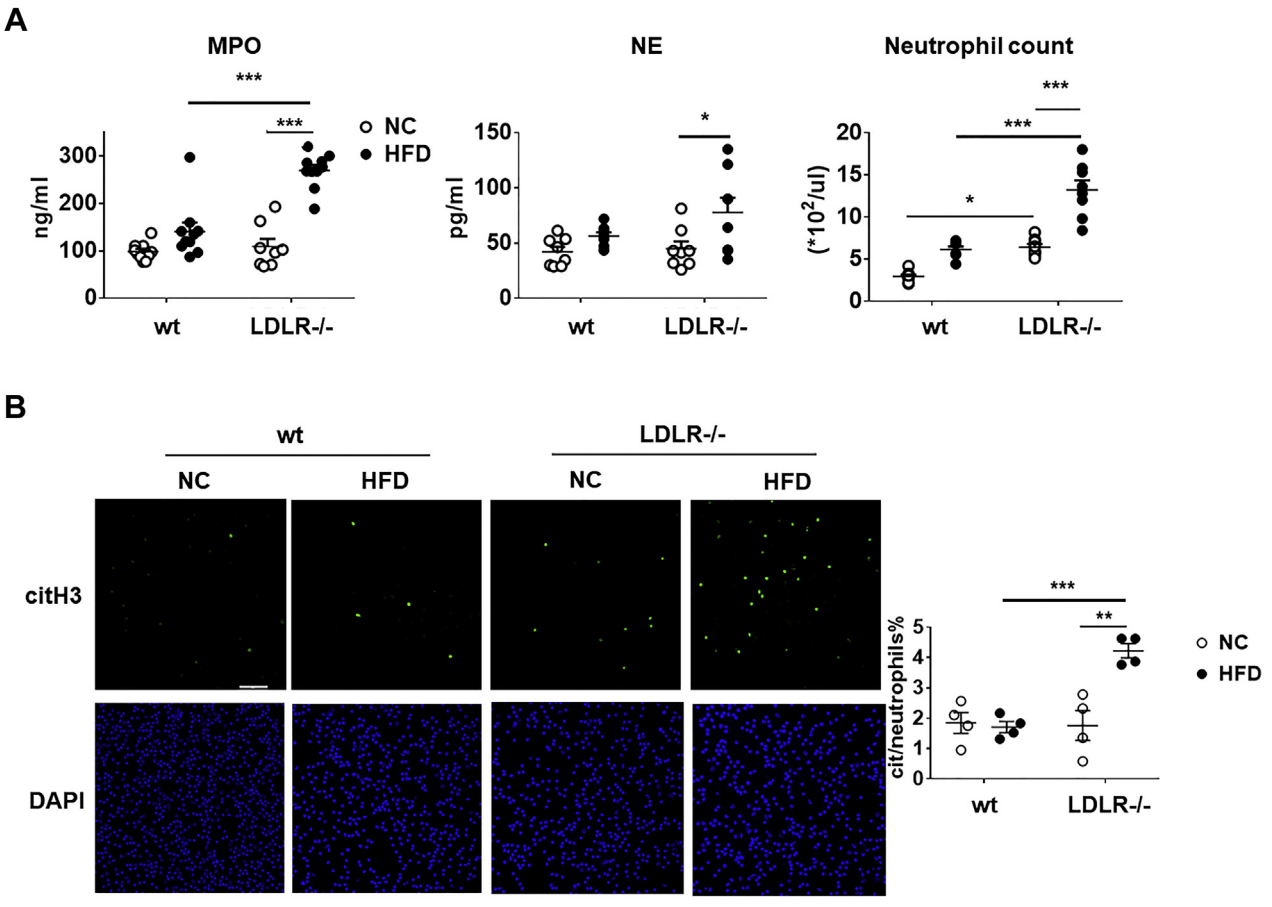

(A) MPO **(left)** and NE **(middle)** levels and neutrophil count **(right)** in the blood of wt mice fed NC or HFD or LDLR$^{-/-}$ mice fed NC or HFD for 28 days. **White circles** indicate NC-fed mice, and **black circles** indicate HFD-fed mice. n = 4 to 8. **(B)** Immunohistochemistry for citrullinated histone H3 in circulating neutrophils of each mouse (n = 4). **Green** indicates citrullinated histone H3, and **blue** indicates nuclei. Scale bar: 50 μm. **The graph (right)** shows the frequency of citrullinated histone H3–positive neutrophils. **White circles** indicate NC, and **black circles** indicate HFD. Data are presented as the mean ± SEM. ***p < 0.001, **p < 0.01, and *p < 0.05 by 2-way ANOVA with the Bonferroni post hoc test. n = 4 in each group. citH3 = citrullinated histone H3; DAPI = 4′,6-diamidino-2-phenylindole; MPO = myeloperoxidase; NE = neutrophil elastase; other abbreviations as in Figure 1.

(approval no. M2000-2205), and we conformed to the principles outlined in the Declaration of Helsinki. Written informed consent was provided by all healthy volunteers older than 20 years before blood was taken. An equal volume of 2% Dextran T-500 (Pharmacosmos A/S, Holbaek, Denmark) in saline was added to peripheral blood drawn from a healthy volunteer with heparin after centrifugation in Ficoll-Paque (Sigma-Aldrich) (35). Approximately 93% of the isolated cells were determined to be CD66b-positive neutrophils by flow cytometry (Supplemental Figure 1).

NONSTATIC ADHESION ASSAY. Human umbilical vein endothelial cells (HUVECs) were purchased from Lonza (Basel, Switzerland) and cultured in RPMI 1640 medium supplemented with 20% fetal bovine serum, 100 unit/ml penicillin, 0.17 nmol/L streptomycin, and 2 mmol/L L-glutamine. HUVECs were seeded on 6-well plates coated with gelatin, and they were stimulated with 0.1 unit/ml of interleukin 1β for 4 hours. Human circulating neutrophils were stimulated with 2 nmol/L or 10 nmol/L CXCL1 (BioLegend, Inc.) or 2 nmol/L or 10 nmol/L TDFA with 10 nmol/L CXCL1 for 2 hours and labeled with 2′,7′-bis-(2-carboxyethyl)-5-(and-6)-carboxyfluorescein acetoxymethyl ester (BCECF-AM, FUJIFILM Wako Pure Chemical Corporation). Moreover, 2 × 10^6 of labeled cells were applied to HUVECs and rotated at 64 revolutions/minute for 10 minutes at room temperature. After washing 3 times, adhered cells were removed with ethylene glycol tetraactic acid/

FIGURE 3 Plasma of LDLR$^{-/-}$ Mice Fed HFD for 28 Days Induced Citrullination of Histone H3 in BM-Neutrophils From LDLR$^{-/-}$ Mice

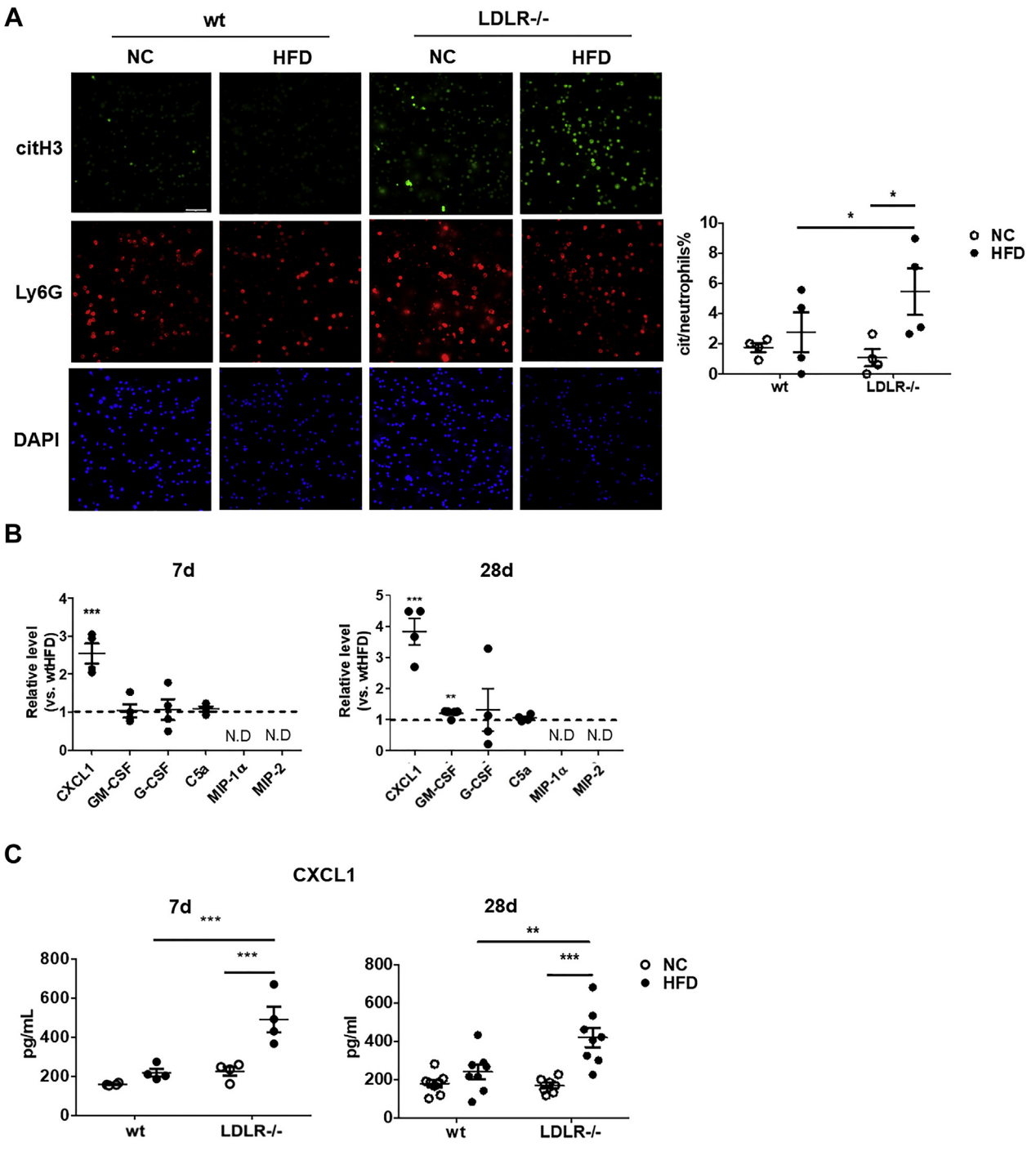

(A) BM-derived leukocytes were stimulated by plasma from wt mice fed NC or HFD or from LDLR$^{-/-}$ mice fed NC or HFD for 28 days following immunohistochemistry for citrullinated histone H3. **Green** indicates citrullinated histone H3, **red** indicates Ly-6G, and **blue** indicates nuclei. Scale bar: 50 μm. **The graph (right)** shows the frequency of citrullinated histone H3-positive neutrophils. **White circles** indicate NC-fed mice, and **black circles** indicate HFD-fed mice. n = 4 in each group. **(B)** Comprehensive analysis for cytokines/chemokines to activate or recruit neutrophil in the plasma of LDLR$^{-/-}$ mice fed HFD for 7 days or 28 days. The relative values for LDLR$^{-/-}$ mice fed HFD were calculated, as the level of wt mice fed HFD was 1. n = 4 in each group. **(C)** CXCL1 levels in plasma of wt mice fed NC or HFD or of LDLR$^{-/-}$ mice fed NC or HFD for 7 days or 28 days. **White circles** show NC, and **black circles** show HFD. n = 4 or 8. Data are presented as the mean ± SEM. ***p < 0.001, **p < 0.01, and *p < 0.05 by 2-way ANOVA with the Bonferroni post hoc test. BM = bone marrow; N.D = not detected; other abbreviations as in Figure 1.

FIGURE 4 **CXCL1 Induced Citrullination of Histone H3 in BM-Neutrophils**

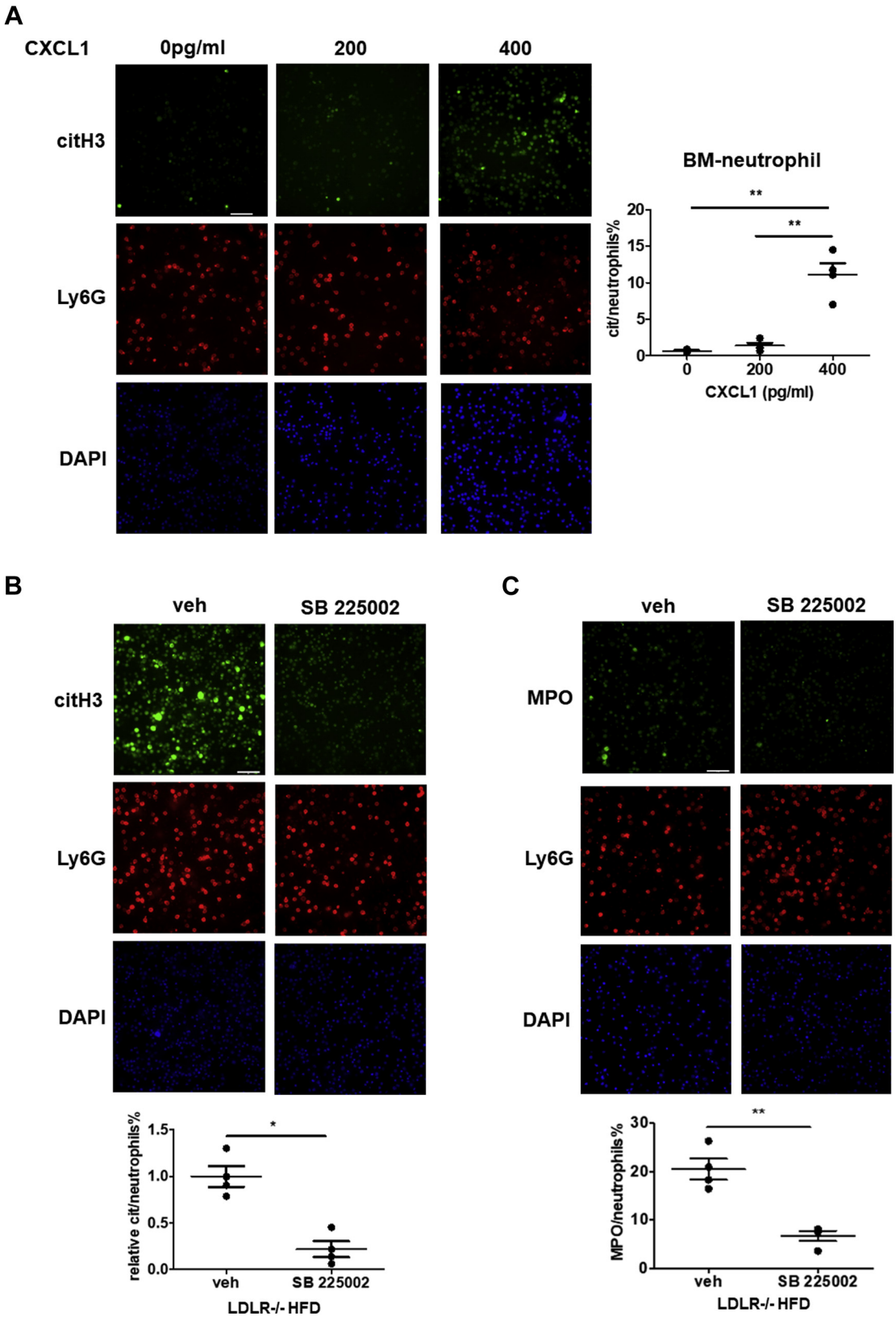

Continued on the next page

FIGURE 4 Continued

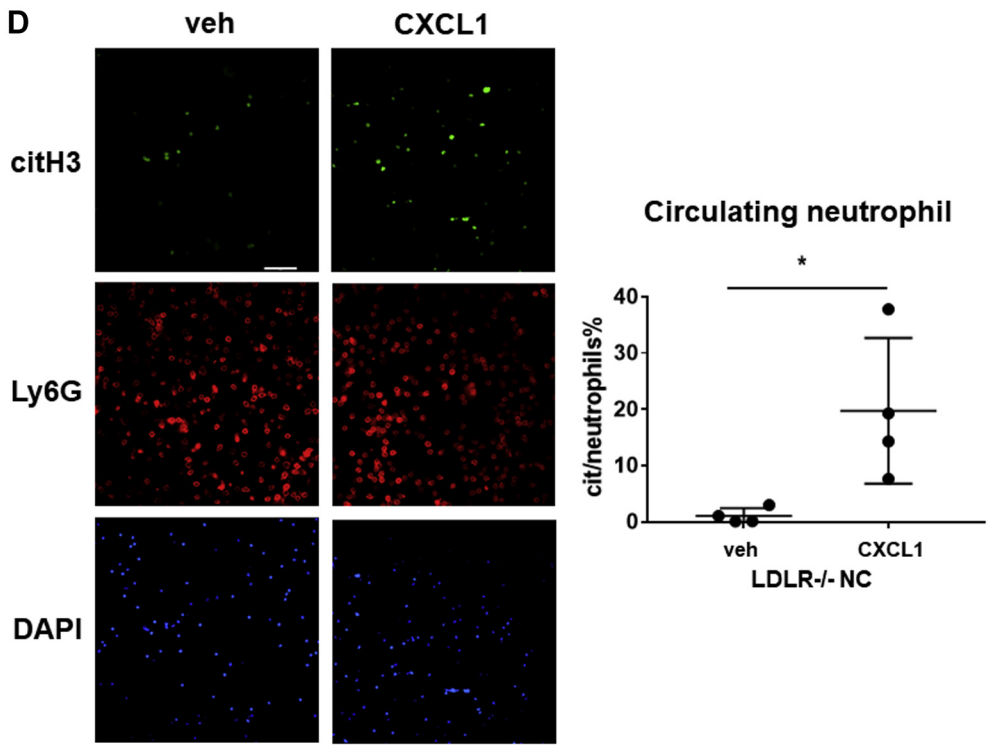

(A) BM-leukocytes were stimulated with 0, 200, and 400 pg/ml CXCL1. Immunohistochemistry for citrullinated histone H3 was performed after 2 hours. **Green** indicates citrullinated histone H3, **red** indicates Ly-6G, and **blue** indicates nuclei. Scale bar: 50 μm. **The graph (right)** shows the frequency of citrullinated histone H3–positive neutrophils. Data are presented as the mean ± SEM. **$p < 0.01$ by 2-way ANOVA with the Bonferroni post hoc test. n = 4 in each group. **(B)** BM-derived leukocytes were stimulated by plasma from $LDLR^{-/-}$ mice fed HFD administered SB225002, which is a CXCR2 antagonist, for 28 days and examined by immunohistochemistry for citrullinated histone H3. **Green** indicates citrullinated histone H3, **red** indicates Ly-6G, and **blue** indicates nuclei. Scale bar: 50 μm. The graph **(right)** shows the frequency of citrullinated histone H3-positive neutrophils. Data are presented as the mean ± SEM. *$p < 0.05$ by unpaired 2-tailed Student's *t*-test. n = 4 in each group. **(C)** Immunohistochemistry for MPO in BM-derived leukocytes by stimulation with plasma from $LDLR^{-/-}$ mice fed HFD administered SB225002. **Green** indicates MPO, **red** indicates Ly-6G, and **blue** indicates nuclei. Scale bar: 50 μm. The graph **(right)** shows the frequency of MPO-positive neutrophils. Data are presented as the mean ± SEM. **$p < 0.01$ by unpaired 2-tailed Student's *t*-test. n = 4 in each group. **(D)** Immunohistochemistry for citrullinated histone H3 in isolated circulating neutrophils stimulated with 400 pg/ml of CXCL1 was examined. **Green** indicates citrullinated histone H3, **red** indicates Ly-6G, and **blue** indicates nuclei. Scale bar: 50 μm. **The graph (right)** shows the frequency of citrullinated histone H3-positive neutrophils. Data are presented as the mean ± SEM. *$p < 0.05$ by unpaired 2-tailed Student's *t*-test. n = 4 in each group. veh = vehicle; other abbreviations as in Figures 1 to 3.

ethylenediaminetetra-acetic acid solution, and these cells were lysed by lysis buffer. The fluorescence intensity of the lysate was measured at 485/535 nm using a plate reader (ARVO X3, Perkin Elmer, Waltham, Massachusetts) (36,37).

STATISTICAL ANALYSIS. Data are expressed as the mean value ± standard error of the mean. Two-way analysis of variance with the Bonferroni post hoc test or unpaired 2-tailed Student's *t*-test was used to estimate statistical significance, with a value of $p < 0.05$ considered to be statistically significant. Data were analyzed using Prism 6 or 7 (GraphPad, San Diego, California).

RESULTS

HFD ENHANCED NEUTROPHIL ADHESION IN $LDLR^{-/-}$ mice. Our previous study reported that HFD induced neutrophil adhesion in wt mice (8). Thus, we first observed neutrophil adhesion in HFD-fed $LDLR^{-/-}$ mice for 28 days and compared the results to those in HFD-fed wt mice by IVM analysis. As shown in Figure 1A, a number of adherent leukocytes were significantly higher in HFD-fed $LDLR^{-/-}$ mice than in HFD-fed wt mice. Furthermore, the frequency of firm adhesion (≥60 s) between leukocytes and the endothelium was increased in HFD-fed $LDLR^{-/-}$ mice

FIGURE 5 **Inhibition of Citrullination Decreased Neutrophil Adhesion In Vivo and In Vitro**

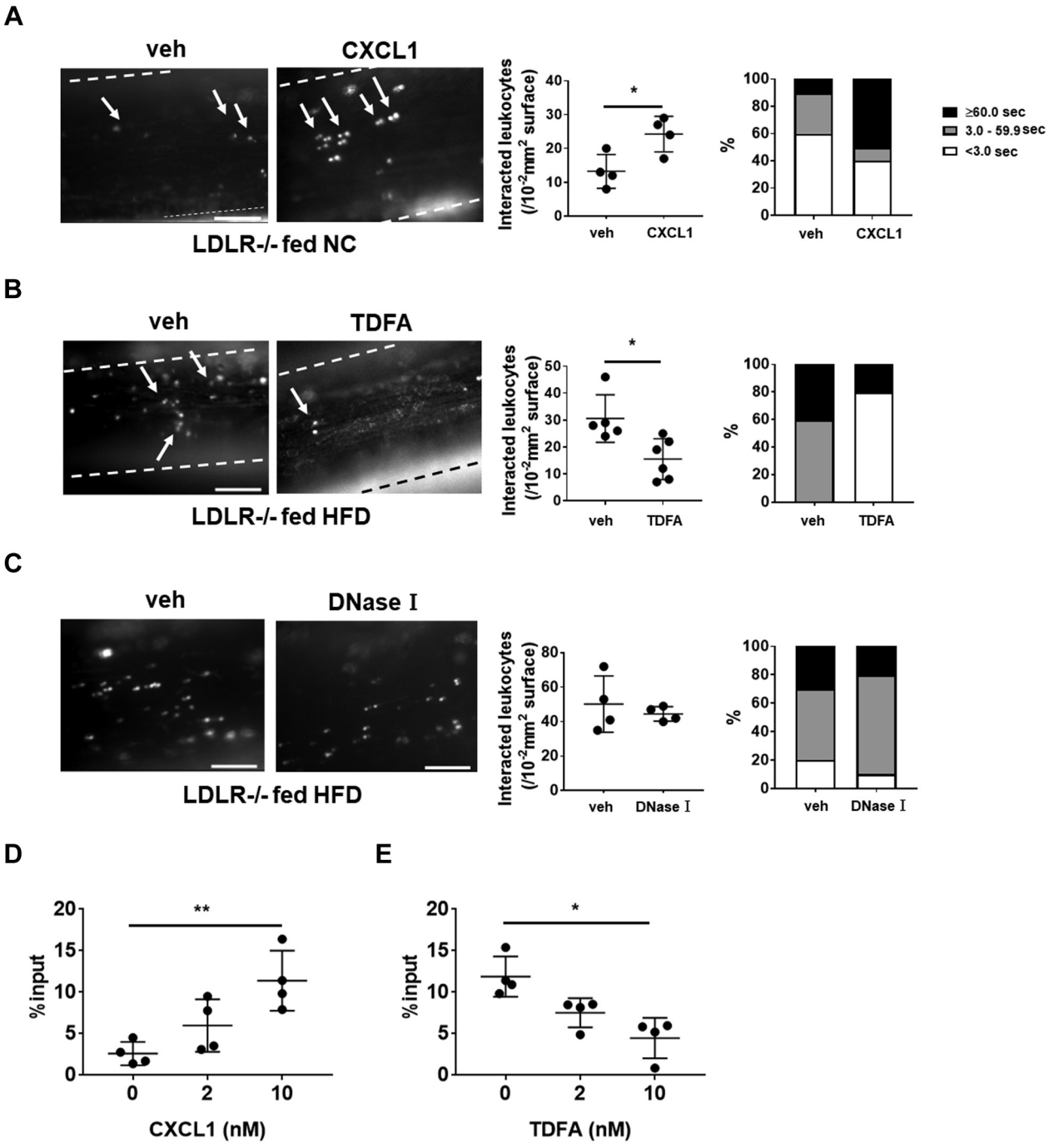

Continued on the next page

compared with that in HFD-fed wt mice. Leukocyte adhesion was observed in LDLR$^{-/-}$ mice fed with NC but not in wt mice (**Figure 1A,** Videos 1-4). Furthermore, TG and TC levels in plasma remarkably increased in LDLR$^{-/-}$ mice fed HFD compared with wt mice fed NC or HFD or LDLR$^{-/-}$ mice fed NC (**Figure 1B**). As we documented in our previous study, we confirmed that the adherent leukocytes were

neutrophils but not other leukocyte subtypes by using LysM-eGFP mice injected with clodronate (8). In the absence of clodronate liposome, the neutrophils and monocytes of LDLR$^{-/-}$ LysM-eGFP mice express GFP (Supplemental Figure 2A). However, when monocytes/macrophages were depleted using clodronate, a GFP signal from LDLR$^{-/-}$ LysM-eGFP mice was undetectable. Then, we used LDLR$^{-/-}$ LysM-eGFP mice depleted monocytes/macrophages, which were undetectable (Supplemental Figure 2B). As presented in **Figure 1A**, HFD feeding significantly increased leukocyte adhesion and firm adhesion (≥60 seconds) in LDLR$^{-/-}$ LysM-eGFP mice compared to NC mice (Videos 5 **and** 6). The result of that methodological approach demonstrated that monocyte depletion did not change leukocyte adhesion in LDLR$^{-/-}$ LysM-eGFP mice (**Figure 1C,** Videos 7 **and** 8), suggesting that HFD actually enhanced the adhesion of neutrophils in LDLR$^{-/-}$ mice.

CITRULLINATION WAS INCREASED IN CIRCULATING NEUTROPHILS IN HFD-FED LDLR$^{-/-}$ MICE. NE and MPO are known markers of NETs (19,38). To characterize NETs in LDLR$^{-/-}$ mice, we measured the NE and MPO levels and the peripheral neutrophil count. The NE and MPO levels and circulating neutrophil count significantly increased in LDLR$^{-/-}$ mice fed HFD compared with wt mice fed HFD or LDLR$^{-/-}$ mice fed NC (**Figure 2A**). Because we hypothesized that NETs are involved in the neutrophil adhesion observed in the HFD-fed LDLR$^{-/-}$ mice, we measured the expression level of citrullinated histone H3 in circulating neutrophils. It was significantly increased in LDLR$^{-/-}$ mice fed HFD compared with wt mice fed NC or HFD or with LDLR$^{-/-}$ mice fed NC (**Figure 2B**).

PLASMA FROM LDLR$^{-/-}$ MICE, BUT NOT WT MICE, FED HFD INDUCED NEUTROPHIL CITRULLINATION. To clarify the mechanisms by which the citrullination of histone H3 was induced in HFD-fed LDLR$^{-/-}$ mice, we examined the effect of plasma taken from LDLR$^{-/-}$ mice or wt mice in the presence or absence of HFD, and the plasma from each mouse was subjected to BM-leukocytes from LDLR$^{-/-}$ mice. The plasma of LDLR$^{-/-}$ mice fed HFD for 28 days significantly induced histone H3 citrullination in BM-leukocytes (**Figure 3A**). Interestingly, the plasma of wt mice fed HFD for 28 days failed to induce histone H3 citrullination, although neutrophil adhesion was induced, suggesting that a distinct pathway may be involved in HFD-induced neutrophil activation in LDLR$^{-/-}$ mice compared with wt mice. BM-leukocytes from wt mice were also induced histone H3 citrullination by the plasma of LDLR$^{-/-}$ mice fed HFD but not wt mice (Supplemental Figure 3). Therefore, these data suggest that histone H3 citrullination depends on plasma components. Moreover, these data show that plasma from HFD-fed LDLR$^{-/-}$ mice, but not from wt mice, contains a factor that induces the citrullination of histone H3.

To identify potential factors that influence the hypercitrullination of histone H3 in LDLR$^{-/-}$ mice, comprehensive cytokine/chemokine analysis for cytokines and chemokines related to neutrophil chemotaxis or activation was conducted using plasma from LDLR$^{-/-}$ mice or wt mice in the presence or absence of HFD. Among the several factors we identified (as shown in **Figure 3B**), the plasma levels of CXCL1 and granulocyte-macrophage colony-stimulating factor (GM-CSF) were specifically and significantly increased in LDLR$^{-/-}$ mice after HFD for 7 and 28 days. Furthermore, enzyme-linked

FIGURE 5 Continued

(A) Leukocyte adhesion were observed in LDLR$^{-/-}$ mice fed NC with 0.3 mg/kg BW of CXCL1 for 2 hours. CXCL1 significantly increased leukocyte adhesion in LDLR$^{-/-}$ mice. **Arrowheads** show adhered leukocytes or rolling leukocytes on the vessel wall, and dashed lines indicate the vessel wall in the snapshot. **The graph (right)** shows the number of adhered/rolling leukocytes. *$p < 0.05$ by unpaired 2-tailed Student's *t*-test. n = 4 in each group. Videos 9 and 10 show in vivo imaging of adhered and rolling leukocytes on the femoral artery of LDLR$^{-/-}$ mice administered or not administered CXCL1. **(B)** Leukocyte adhesion on the femoral artery of LDLR$^{-/-}$ mice fed HFD administered TDFA for 28 days. **The graph (right)** shows the number of adhered/rolling leukocytes. Scale bar: 50 μm. Data are presented as the mean ± SEM. *$p < 0.05$ by unpaired 2-tailed Student's *t*-test. n = 5 or 6. Videos 11 and 12 show in vivo imaging of adhered and rolling leukocytes on the femoral artery of HFD-fed LDLR$^{-/-}$ mice administered or not administered TDFA. **(C)** Leukocyte adhesion on the femoral artery of LDLR$^{-/-}$ mice fed HFD administered 0.2 mg of DNaseI for 7 days before IVM. DNaseI did not change leukocyte adhesion in these mice. **The graph (right)** shows the number of adhered/rolling leukocytes. Scale bar: 50 μm. Data are presented as the mean ± SEM. *$p < 0.05$ by unpaired 2-tailed Student's *t*-test. n = 4 in each group. Videos 13 and 14 show in vivo imaging of adhered and rolling leukocytes on the femoral artery of LDLR$^{-/-}$ mice administered or not administered DNaseI. **(D)** Treatment of CXCL1 to human peripheral neutrophils increased neutrophil adhesion to HUVECs stimulated with interleukin 1b in a concentration-dependent manner. n = 4 in each group. **(E)** Treatment of 10 nmol/L of TDFA to human peripheral neutrophils stimulated with 10 nmol/L CXCL1 decreased neutrophil adhesion to HUVECs in a concentration-dependent manner. Data are presented as the mean ± SD. **$p < 0.01$ and *$p < 0.05$ by 2-way ANOVA with the Bonferroni post hoc test. n = 4 in each group. BW = body weight; DNaseI = deoxyribonuclease I; HUVECs = human umbilical vein endothelial cells; IVM = intravital microscopy; M = mol/L; TDFA = *N*-acetyl-L-threonyl-L-α-aspartyl-*N*5-(2-fluoro-1-iminoethyl)-L-ornithinamide trifluoroacetate salt; other abbreviations as in **Figures 1 and 4**.

FIGURE 6 **Pemafibrate Improved Neutrophil Adhesion and Citrullination in LDLR$^{-/-}$ Mice Fed HFD**

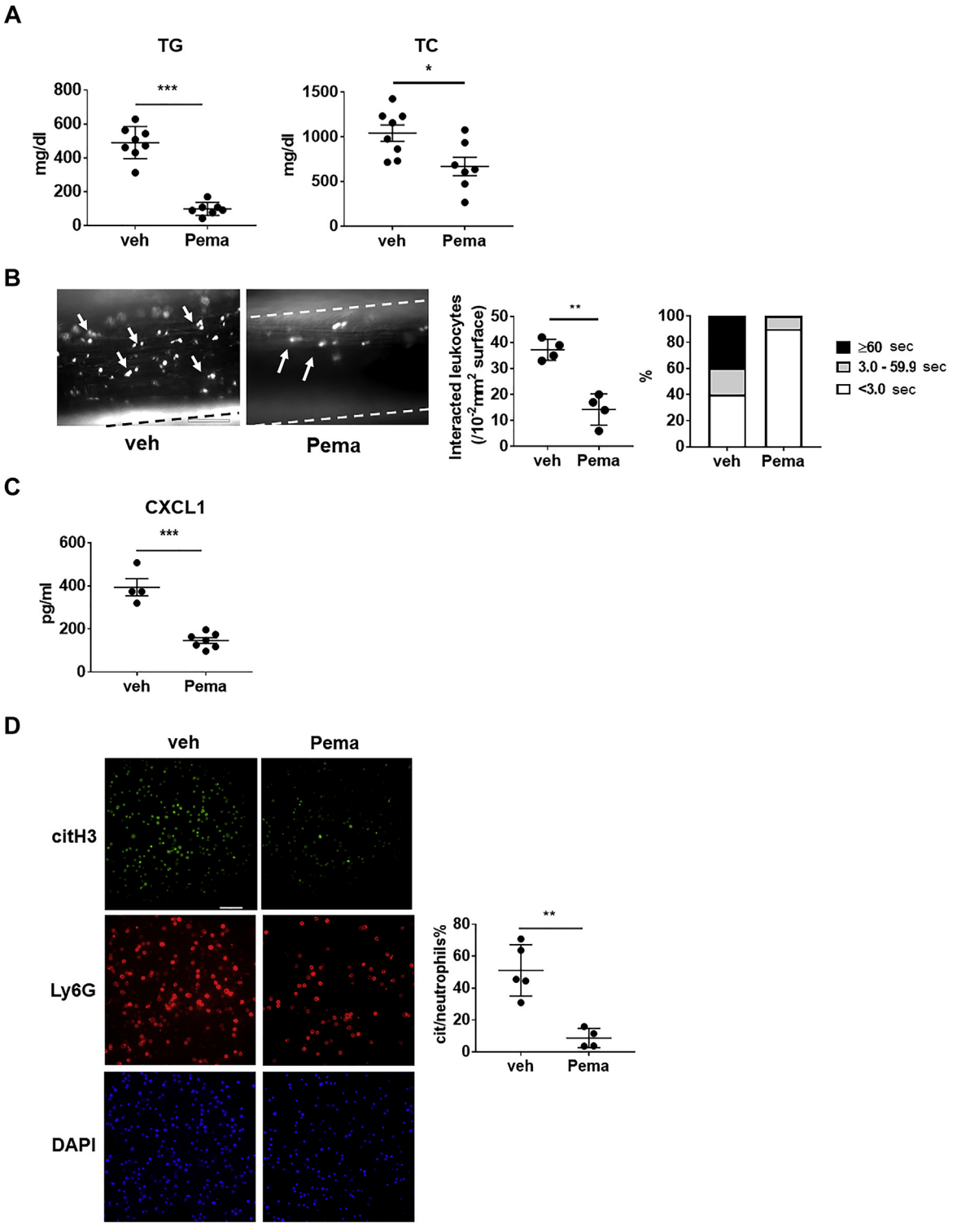

Continued on the next page

immunosorbent assay showed that CXCL1 or GM-CSF significantly increased in LDLR$^{-/-}$ mice fed HFD for 28 days compared with other mice (**Figure 3C,** Supplemental Figure 4A).

CXCL1, BUT NOT GM-CSF, INDUCED NEUTROPHIL CITRULLINATION. To clarify the potential effects of CXCL1 or GM-CSF to induce citrullination of histone H3, we performed immunohistochemistry for citrullinated histone H3 in BM-leukocytes stimulated by CXCL1 and GM-CSF. Moreover, 400 pg/ml of CXCL1 (the concentration in the plasma of LDLR$^{-/-}$ mice fed HFD) significantly induced citrullination compared with the effects of 200 pg/ml CXCL1 (the concentration in the plasma of HFD-fed wt mice) (**Figure 4A**). However, 100 pg/ml GM-CSF (the concentration in the plasma of HFD-fed LDLR$^{-/-}$ mice) did not induce histone H3 citrullination in BM-leukocytes compared with 10 pg/ml of GM-CSF, the plasma concentration in wt mice fed HFD (Supplemental Figure 4B).

When the plasma of HFD-fed LDLR$^{-/-}$ mice treated with CXCR2 antagonist SB225002 (to block CXCL1-CXCR2-dependent signaling) was used, the citrullination of histone H3 in BM-leukocytes was significantly reduced compared with plasma treated with vehicle (**Figure 4B**). However, the plasma of HFD-fed LDLR$^{-/-}$ mice treated with anti-GM-CSF antibody failed to modify the citrullination of histone H3 in BM-leukocytes (Supplemental Figure 4C). These results indicate that CXCL1, but not GM-CSF, induces citrullination in the neutrophils of LDLR$^{-/-}$ mice fed HFD. Moreover, SB225002 treatment significantly reduced the expression of MPO in neutrophils (**Figure 4C**), suggesting a pivotal role for CXCL1-CXCR2 signaling in HFD-induced activation of neutrophils in LDLR$^{-/-}$ mice.

Furthermore, citrullination in the circulating neutrophils of LDLR$^{-/-}$ mice administered CXCL1 was significantly enhanced in comparison with vehicle treatment (**Figure 4D**). These results indicate that the elevation of CXCL1 in blood induces the citrullination of histone H3 in the circulating neutrophils of LDLR$^{-/-}$ mice.

NEUTROPHIL CITRULLINATION WAS RESPONSIBLE FOR NEUTROPHIL ADHESION IN VIVO AND IN VITRO. To monitor whether CXCL1 alone can induce neutrophil adhesion in vivo, we performed IVM analysis using LDLR$^{-/-}$ in the absence of HFD. The administration of CXCL1 significantly increased neutrophil adhesion and firm adhesion (≧60 s) in the femoral artery of LDLR$^{-/-}$ mice in the absence of HFD (**Figure 5A,** Videos 9 and 10). To investigate whether the citrullination of histone H3 is necessary for HFD-induced neutrophil adhesion in vivo, we performed IVM for LDLR$^{-/-}$ mice fed HFD with or without TDFA, a selective PAD4 inhibitor. The administration of TDFA significantly decreased leukocyte adhesion in LDLR$^{-/-}$ mice fed HFD (**Figure 5B,** Supplemental Figure 5, Videos 11 and 12). Furthermore, neutrophil adhesion was examined in HFD-fed LDLR$^{-/-}$ mice administered deoxyribonuclease I (DNaseI) to investigate the involvement of NETosis in neutrophil adhesion. DNaseI did not change neutrophil adhesion in these mice (**Figure 5C,** Videos 13 and 14). These results indicate that citrullination in neutrophils, but not chromatin release in NETosis, is involved in neutrophil adhesion by CXCL1.

To demonstrate the effect of CXCL1 in vitro, non-static adhesion assay using human neutrophils and interleukin 1b-activated HUVECs was performed. As shown in **Figure 5D**, CXCL1 significantly increased the adhesion of neutrophils to endothelial cells in a concentration-dependent manner. When we performed non-static adhesion assay using human neutrophils with or without TDFA, TDFA significantly reduced adherent neutrophils in a concentration-dependent manner (**Figure 5E**). These data suggest that the inhibition of citrullination in neutrophils reduced neutrophil adhesion to endothelial cells by CXCL1 stimulation.

SELECTIVE PPARα MODULATOR PEMAFIBRATE DECREASED NEUTROPHIL ADHESION AND CITRULLINATION OF HISTONE H3 THROUGH REDUCTION OF CXCL1. Citrullination in wt mice fed HFD did not change, with no increase of TG levels in blood. However, TG levels and citrullination

FIGURE 6 Continued

(A) Plasma TG and TC levels in LDLR$^{-/-}$ mice fed HFD with or without pemafibrate. Pemafibrate improved hypertriglyceridemia and hypercholesterolemia. n = 7 or 8. **(B)** Pemafibrate decreased neutrophil adhesion in LDLR$^{-/-}$ mice fed HFD. **Arrowheads** show adhered leukocytes or rolling leukocytes on the vessel wall, and **dashed** lines indicate the vessel wall in the snapshot. Scale bar: 50 μm. **The graph (right)** shows the number of adhered leukocytes in each mouse. Data are presented as the mean ± SEM, by unpaired 2-tailed Student's *t*-test. n = 4 each group. Videos 15 and 16 show in vivo imaging of the adhered and rolling leukocytes on the femoral artery of LDLR$^{-/-}$ mice administered or not administered pemafibrate. **(C)** CXCL1 level in the plasma of LDLR$^{-/-}$ mice fed HFD with or without pemafibrate. Pemafibrate decreased CXCL1 level. n = 4 or 7. **(D)** Immunohistochemistry for citrullinated histone H3 by stimulation with plasma from LDLR$^{-/-}$ mice administered or not administered pemafibrate. **Green** indicates citrullinated histone H3, **red** indicates Ly6G, and **blue** indicates nuclei. Scale bar: 50 μm. **The graph (right)** shows the frequency of citrullinated histone H3-positive neutrophils. n = 5 or 4. Data are presented as the mean ± SEM. ***$p < 0.001$, **$p < 0.01$, and *$p < 0.05$ by unpaired 2-tailed Student's *t*-test. Pema = pemafibrate; other abbreviations as in **Figures 1 to 4**.

were enhanced in LDLR$^{-/-}$ mice fed HFD (**Figure 1B and 2B**). Taking these data together, we hypothesized that the increment of TG in blood is involved in neutrophil adhesion and the citrullination of neutrophils. Hence, we examined neutrophil adhesion and citrullination in LDLR mice fed HFD by the administration of pemafibrate (K-877), which is a novel selective PPARα modulator that has a TG-lowering effect in blood. Pemafibrate, remarkably, decreased TG and TC levels in LDLR$^{-/-}$ mice fed HFD (**Figure 6A**). Moreover, pemafibrate significantly reduced neutrophil adhesion, CXCL1 levels in blood, and citrullination levels in circulating neutrophils without changing the neutrophil count versus the vehicle (**Figure 6B-D,** Supplemental Figure 6A, Videos 15 and 16). These results indicate that pemafibrate improves dyslipidemia, systemic inflammation, and neutrophil activation by HFD.

DISCUSSION

In this study, we reported that the citrullination of histone H3 by CXCL1 is involved in enhanced neutrophil adhesion in the femoral artery of LDLR$^{-/-}$ mice fed HFD. Vascular inflammation is integral to the development of atherosclerosis (13). Previous studies have provided some lines of evidence to show that monocytes/macrophages are key players in this chronic inflammatory disease (39). In general, the initiation of inflammation is mediated by neutrophils that function to minimally activate the intracellular machinery to maintain the homeostatic functions of the tissue. However, when an inflammatory agent elicits a strong and/or persistent response, these initial acute responses can shift toward a more complex and prolonged process mediated by mononuclear cells, including lymphocytes and monocytes/macrophages (40). We propose that this theory is operative in the case of atherosclerosis, with dyslipidemia as a persistent inflammatory stimulus. To this end, we tried to document the potential roles of neutrophils during acute inflammation in atherosclerosis. We have previously reported the importance of neutrophils in HFD-induced vascular inflammation in wt mice. Thus, we extend that notion to atherosclerosis using LDLR$^{-/-}$ mice, a relevant model for HFD-induced atherosclerosis. As shown in **Figure 1**, HFD induced prominent inflammation primarily via neutrophils in LDLR$^{-/-}$ mice with a significant elevation of plasma TG and cholesterol levels when compared with wt mice. In fact, the enhancement of NE and MPO levels in LDLR$^{-/-}$ mice fed HFD indicated that neutrophil activation is more striking in LDLR$^{-/-}$ mice. Because the up-regulation of NE or MPO is also a marker of NETs (19,38), we then hypothesized that distinct mechanism(s) such as NETs may be involved in the HFD-induced neutrophil activation observed in LDLR$^{-/-}$ mice but not in wt mice. Neutrophils have functions such as the detection of infection and phagocytosis in the innate immune system (9). In addition, NETs and NET formation help trap bacteria and fungi to eliminate pathogens from the host (41). NET is a chromatin filament structure including DNA, histones, proteases, and secreted granule proteins such as NE and MPO. Invading bacteria, fungi, and viruses are captured by NETs and killed with granule proteins in NETs (42). NETs are formed after the conversion of arginine residue to citrulline in histones; hence, citrullinated histone H3 is widely accepted as a marker of NETs (43). We showed that more citrullinated histone H3 is present in the circulating neutrophils of LDLR$^{-/-}$ mice compared with wt mice fed HFD after 28 days (**Figure 2B**). Furthermore, leukocyte adhesion was enhanced in LDLR$^{-/-}$ mice fed HFD (**Figure 1A**). These results suggest the involvement of histone citrullination and NETs in neutrophil adhesion in LDLR$^{-/-}$ mice fed HFD.

To further characterize the leukocyte subtype that is involved, we used LDLR$^{-/-}$ LysM-eGFP mice administered clodronate liposomes, which are depleted monocytes but not neutrophils, to specifically monitor neutrophils. As shown in **Figure 1C**, comparable levels of neutrophil adhesion in these mice were induced by HFD. Furthermore, pemafibrate suppressed neutrophil adhesion without change of the neutrophil count in blood (**Figure 6A**). Therefore, these results indicate that neutrophils are activated in LDLR$^{-/-}$ mice fed HFD. Additionally, enhanced neutrophil adhesion was significantly reduced by the administration of TDFA, which inhibits the citrullination of histones through down-regulation of PAD4 activity (34) (**Figure 5B**), suggesting the involvement of histone citrullination and NETs in neutrophil adhesion. Interestingly, however, the administration of DNaseI, an agent that blocks the NET-related extracellular DNA/chromatin network (44,45), failed to alter the level of leukocyte adhesion in LDLR$^{-/-}$ mice (**Figure 5C**). A recent report indicated that suicidal NETs induce the death of neutrophils through the disruption of the DNA-chromatin complex which is sensitive to DNaseI, whereas vital NETs have functions such as phagocytosis, chemotaxis, and permeability without destruction of the DNA-chromatin and are resistant to DNaseI (46). This observation suggests that vital NETs, rather than suicidal NETs, may be involved in HFD-induced vascular inflammation in LDLR$^{-/-}$ mice.

Another recent observation suggests the involvement of NETs in atherosclerosis-related vascular events such as plaque rupture and thrombosis-

induced endothelial cell dysfunction (47). In another report, the inhibition of NET formation by the transplantation of PAD4-deficient BM-derived cells or the administration of DNaseI reduced arterial endothelial damage in the artery injury model (48). Our data indicate that PAD4 plays a role in HFD-induced vascular inflammation.

In this paper, we have been able to identify CXCL1 as a potential key factor that links HFD to hypercitrullination (**Figure 4D**). The administration of CXCL1 alone is enough to reconstitute HFD-mediated vascular inflammation in LDLR$^{-/-}$ mice (**Figure 5A**). CXCL1 is a CXC chemokine, which is known as a keratinocyte-derived chemokine in mice and as a growth-regulated oncogene alpha in humans. CXCL1-CXCR2 signaling has been shown to play a role in inflammatory diseases such as infection, traumatic brain injury, and multiple sclerosis (49). Furthermore, growth-regulated oncogene alpha levels are increased in the blood of patients with angina (50), suggesting that histone citrullination in peripheral blood is enhanced in patients with atherosclerosis. We would like to investigate the molecular mechanisms of the induction of hypercitrullination by CXCL1 in our future study.

Pemafibrate (K-877) is a novel selective PPARα modulator, which is the treatment for dyslipidemia. PPARα promotes not only the activation of β oxidation and transcription of the lipoprotein lipase gene but also the reduction of ApoC-III expression, leading to lower TG levels (28). In addition, pemafibrate presented anti-inflammatory and antiatherosclerotic effects in mice (27). In fact, pemafibrate decreased the levels of TG, TC, and inflammatory chemokines such as CXCL1, GM-CSF, and C5a that were elevated in the blood of LDLR$^{-/-}$ mice (**Figure 6A and C,** Supplemental Figure 6B). Furthermore, pemafibrate decreased neutrophil adhesion and suppressed citrullination without changing neutrophil count in the blood of LDLR$^{-/-}$ mice (**Figure 6B and D,** Supplemental Figure 6A). To summarize our findings, dyslipidemia might influence the citrullination of histone H3 in neutrophils through CXCL1 up-regulation in blood.

STUDY LIMITATIONS. First, atherosclerotic plaque formation will be assessed using a prolonged HFD-fed mouse model. Second, the contribution of neutrophil citrullination in humans should be examined using an ample number of clinical specimens in a future study.

CONCLUSIONS

Neutrophils play a crucial role in the acute phase of inflammation by infection or injury. Vascular inflammation for the development of atherosclerosis closely involves inflammation. Therefore, it is considered to form the acute phase and chronic phase of inflammation. Our finding that hypercitrullination was induced in LDLR$^{-/-}$ mice fed HFD but not in wt mice fed HFD may indicate that hypercitrullination and NETs are key factors that facilitate the transition from acute to chronic inflammation.

In conclusion, we demonstrated that HFD induced the hypercitrullination of neutrophils via an CXCL1-mediated pathway specifically in LDLR$^{-/-}$ mice. The elucidation of this process will shed additional light on the initiation of atherosclerosis and the transition from the acute to the chronic phase of vascular inflammation.

ACKNOWLEDGMENTS Dr. Masaki Honda (Kumamoto University) and Dr. Yukihiro Inomata (Kumamoto University) provided LysM-eGFP mice. Pemafibrate was kindly gifted from Kowa Corp. Ltd. We thank the other members in our laboratory for helpful advice.

FUNDING SUPPORT AND AUTHOR DISCLOSURES

This work was supported by a Grant-in-Aid for Exploratory Research (16K15439 to Dr. Yoshida) and a Grant-in-Aid for Scientific Research (C) (15K09153 to Dr. Oaska; and 19K08511 to Dr. Yoshida). The authors have reported that they have no relationships relevant to the contents of this paper to disclose.

ADDRESS FOR CORRESPONDENCE: Dr. Masayuki Yoshida, Department of Life Sciences and Bioethics, Graduate School of Medical and Dental Sciences, Tokyo Medical and Dental University, 1-5-45, Yushima, Bunkyo-ku, Tokyo 113-8519, Japan. E-mail: masa.vasc@tmd.ac.jp.

PERSPECTIVES

COMPETENCY IN MEDICAL KNOWLEDGE: Previous studies have provided lines of evidence to show that monocytes/macrophages are key players in atherosclerotic cardiovascular diseases (ASCVD). This study, however, clarified the contribution of neutrophils via histone H3 citrullination in the acute phase of HFD-induced vascular inflammation with elevation of serum CXCL1. Moreover, elevation of serum TG level, and its resolution by pemafibrate, may regulate the observed neutrophil activation, suggesting a clinical importance of neutrophil activation and serum TG levels in the evaluation of the inflammatory aspect of ASCVD.

TRANSLATIONAL OUTLOOK: This study has linked hypertriglyceridemia and neutrophil activation and the beneficial effects of pemafibrate using a mouse model of atherosclerosis. Therefore, it is important to consider clinical trials or global observations to monitor our findings to initiate new diagnostic tools and treatments for ASCVD.

REFERENCES

1. Hennig B, Toborek M, McClain CJ. High-energy diets, fatty acids and endothelial cell function: implications for atherosclerosis. J Am Coll Nutr 2001;20:97–105.

2. Tomaino RM, Decker EA. High-fat meals and endothelial function. Nutr Rev 1998;56:182–5.

3. Sandesara PB, Virani SS, Fazio S, Shapiro MD. The forgotten lipids: triglycerides, remnant cholesterol, and atherosclerotic cardiovascular disease risk. Endocr Rev 2019;40:537–57.

4. Tada H, Nohara A, Inazu A, Sakuma N, Mabuchi H, Kawashiri MA. Sitosterolemia, hypercholesterolemia, and coronary artery disease. J Atheroscler Thromb 2018;25:783–9.

5. Basu A, Devaraj S, Jialal I. Dietary factors that promote or retard inflammation. Arterioscler Thromb Vasc Biol 2006;26:995–1001.

6. Esposito K, Giugliano D. Diet and inflammation: a link to metabolic and cardiovascular diseases. Eur Heart J 2006;27:15–20.

7. Zhao Y, Yang Y, Xing R, et al. Hyperlipidemia induces typical atherosclerosis development in Ldlr and Apoe deficient rats. Atherosclerosis 2018;271:26–35.

8. Osaka M, Ito S, Honda M, Inomata Y, Egashira K, Yoshida M. Critical role of the C5a-activated neutrophils in high-fat diet-induced vascular inflammation. Sci Rep 2016;6:21391.

9. Kolaczkowska E, Kubes P. Neutrophil recruitment and function in health and inflammation. Nat Rev Immunol 2013;13:159–75.

10. Kourtzelis I, Mitroulis I, von Renesse J, Hajishengallis G, Chavakis T. From leukocyte recruitment to resolution of inflammation: the cardinal role of integrins. J Leukoc Biol 2017;102:677–83.

11. Costa S, Bevilacqua D, Cassatella MA, Scapini P. Recent advances on the crosstalk between neutrophils and B or T lymphocytes. Immunology 2019;156:23–32.

12. Emini Veseli B, Perrotta P, De Meyer GRA, et al. Animal models of atherosclerosis. Eur J Pharmacol 2017;816:3–13.

13. Ross R. Atherosclerosis—an inflammatory disease. N Engl J Med 1999;340:115–26.

14. Hansson GK. Inflammation and immune response in atherosclerosis. Curr Atheroscler Rep 1999;1:150–5.

15. Libby P, Lichtman AH, Hansson GK. Immune effector mechanisms implicated in atherosclerosis: from mice to humans. Immunity 2013;38:1092–104.

16. Brinkmann V, Zychlinsky A. Beneficial suicide: why neutrophils die to make NETs. Nat Rev Microbiol 2007;5:577–82.

17. Meier A, Chien J, Hobohm L, Patras KA, Nizet V, Corriden R. Inhibition of human neutrophil extracellular trap (NET) production by propofol and lipid emulsion. Front Pharmacol 2019;10:323.

18. Demers M, Krause DS, Schatzberg D, et al. Cancers predispose neutrophils to release extracellular DNA traps that contribute to cancer-associated thrombosis. Proc Natl Acad Sci U S A 2012;109:13076–81.

19. Papayannopoulos V, Metzler KD, Hakkim A, Zychlinsky A. Neutrophil elastase and myeloperoxidase regulate the formation of neutrophil extracellular traps. J Cell Biol 2010;191:677–91.

20. Nakashima K, Arai S, Suzuki A, et al. PAD4 regulates proliferation of multipotent haematopoietic cells by controlling c-myc expression. Nat Commun 2013;4:1836.

21. Tilvawala R, Thompson PR. Peptidyl arginine deiminases: detection and functional analysis of protein citrullination. Curr Opin Struct Biol 2019;59:205–15.

22. Li P, Wang D, Yao H, et al. Coordination of PAD4 and HDAC2 in the regulation of p53-target gene expression. Oncogene 2010;29:3153–62.

23. Xiao S, Lu J, Sridhar B, et al. SMARCAD1 contributes to the regulation of naive pluripotency by interacting with histone citrullination. Cell Rep 2017;18:3117–28.

24. Sørensen OE, Borregaard N. Neutrophil extracellular traps—the dark side of neutrophils. J Clin Invest 2016;126:1612–20.

25. Ganda OP, Bhatt DL, Mason RP, Miller M, Boden WE. Unmet need for adjunctive dyslipidemia therapy in hypertriglyceridemia management. J Am Coll Cardiol 2018;72:330–43.

26. Shapiro MD, Fazio S. From lipids to inflammation: new approaches to reducing atherosclerotic risk. Circ Res 2016;118:732–49.

27. Hennuyer N, Duplan I, Paquet C, et al. The novel selective PPARα modulator (SPPARMα) pemafibrate improves dyslipidemia, enhances reverse cholesterol transport and decreases inflammation and atherosclerosis. Atherosclerosis 2016;249:200–8.

28. Sasaki Y, Raza-Iqbal S, Tanaka T, et al. Gene expression profiles induced by a novel selective peroxisome proliferator-activated receptor α modulator (SPPARMα) pemafibrate. Int J Mol Sci 2019;20:5682.

29. Faust N, Varas F, Kelly LM, Heck S, Graf T. Insertion of enhanced green fluorescent protein into the lysozyme gene creates mice with green fluorescent granulocytes and macrophages. Blood 2000;96:719–26.

30. Osaka M, Hagita S, Haraguchi M, Kajimura M, Suematsu M, Yoshida M. Real-time imaging of mechanically injured femoral artery in mice reveals a biphasic pattern of leukocyte accumulation. Am J Physiol Heart Circ Physiol 2007;292:H1876–82.

31. Osaka M, Hagita S, Yoshida M. *In vivo* imaging of leukocyte recruitment to the atheroprone femoral artery reveals anti-inflammatory effects of rosuvastatin. Biomed Res Int 2013;2013:962369.

32. Knight JS, Zhao W, Luo W, et al. Peptidylarginine deiminase inhibition is immunomodulatory and vasculoprotective in murine lupus. J Clin Invest 2013;123:2981–93.

33. White JR, Lee JM, Young PR, et al. Identification of a potent, selective non-peptide CXCR2 antagonist that inhibits interleukin-8-induced neutrophil migration. J Biol Chem 1998;273:10095–8.

34. Jones JE, Slack JL, Fang P, et al. Synthesis and screening of a haloacetamidine containing library to identify PAD4 selective inhibitors. ACS Chem Biol 2012;7:160–5.

35. Böyum A. A one-stage procedure for isolation of granulocytes and lymphocytes from human blood. General sedimentation properties of white blood cells in a 1g gravity field. Scand J Clin Lab Invest Suppl 1968;97:51–76.

36. Yoshida M, Westlin WF, Wang N, et al. Leukocyte adhesion to vascular endothelium induces E-selectin linkage to the actin cytoskeleton. J Cell Biol 1996;133:445–55.

37. Ito S, Osaka M, Edamatsu T, Itoh Y, Yoshida M. Crucial role of the aryl hydrocarbon receptor (AhR) in indoxyl sulfate-induced vascular inflammation. J Atheroscler Thromb 2016;23:960–75.

38. Dwivedi N, Radic M. Citrullination of autoantigens implicates NETosis in the induction of autoimmunity. Ann Rheum Dis 2014;73:483–91.

39. Kimball A, Schaller M, Joshi A, et al. Ly6C(Hi) blood monocyte/macrophage drive chronic inflammation and impair wound healing in diabetes mellitus. Arterioscler Thromb Vasc Biol 2018;38:1102–14.

40. Sansbury BE, Spite M. Resolution of acute inflammation and the role of resolvins in immunity, thrombosis, and vascular biology. Circ Res 2016;119:113–30.

41. Floyd M, Winn M, Cullen C, et al. Swimming motility mediates the formation of neutrophil extracellular traps induced by flagellated pseudomonas aeruginosa. PLoS Pathog 2016;12:e1005987.

42. Munoz Caro T, Hermosilla C, Silva LM, Cortes H, Taubert A. Neutrophil extracellular traps as innate immune reaction against the emerging apicomplexan parasite *Besnoitia besnoiti*. PLoS One 2014;9:e91415.

43. Li P, Li M, Lindberg MR, Kennett MJ, Xiong N, Wang Y. PAD4 is essential for antibacterial innate immunity mediated by neutrophil extracellular traps. J Exp Med 2010;207:1853–62.

44. Lefrancais E, Mallavia B, Zhuo H, Calfee CS, Looney MR. Maladaptive role of neutrophil extracellular traps in pathogen-induced lung injury. JCI Insight 2018;3:e98178.

45. Masuda S, Nonokawa M, Futamata E, et al. Formation and disordered degradation of neutrophil extracellular traps in necrotizing lesions of anti-neutrophil cytoplasmic antibody-associated vasculitis. Am J Pathol 2019;189:839–46.

46. Jorch SK, Kubes P. An emerging role for neutrophil extracellular traps in noninfectious disease. Nat Med 2017;23:279–87.

47. Folco EJ, Mawson TL, Vromman A, et al. Neutrophil extracellular traps induce endothelial cell activation and tissue factor production through interleukin-1alpha and cathepsin G. Arterioscler Thromb Vasc Biol 2018;38:1901–12.

48. Franck G, Mawson TL, Folco EJ, et al. Roles of PAD4 and NETosis in experimental atherosclerosis and arterial injury: implications for superficial erosion. Circ Res 2018;123:33–42.

49. Wu F, Zhao Y, Jiao T, et al. CXCR2 is essential for cerebral endothelial activation and leukocyte recruitment during neuroinflammation. J Neuroinflammation 2015;12:98.

50. Breland UM, Halvorsen B, Hol J, Øie E, Paulsson-Berne G, Yndestad A, et al. A potential role of the CXC chemokine GROalpha in atherosclerosis and plaque destabilization: downregulatory effects of statins. Arterioscler Thromb Vasc Biol 2008;28:1005–11.

KEY WORDS citrullination, cxcl1, in vivo imaging, neutrophil, vascular inflammation

APPENDIX For supplemental videos, figures, and a table, please see the online version of this paper.